

**MODEL ANALYSIS OF A
SKEWED RIGID-FRAME BRIDGE**

by
Ching Sheng Wu

Thesis submitted to the Graduate Faculty of the
Virginia Polytechnic Institute
in candidacy for the degree of

MASTER OF SCIENCE
in
APPLIED MECHANICS

APPROVED:

Director of Graduate Studies

APPROVED:

Head of Department

Dean of Engineering

Major Professor

August, 1955
Blacksburg, Virginia

TABLE OF CONTENTS

I	List of Figures and Tables	3-4
II	Symbols	5
III	Introduction	6
IV	Review of Literature	8
V	Experimental Investigation	10
	1. Object of the Investigation	10
	2. Construction of the Model	10
	3. Testing Frame	18
	4. Method of Testing	19
	5. Reinforcing	23
VI	Data and Results	
	1. Stress and Strain in the Reinforcing	29
	2. Calculation of Principal Strains from the Type AR-2 Rosette Gages	29
VII	Conclusions	38
VIII	Recommendations	39
IX	Bibliography	40
X	Acknowledgements	42
XI	Vita	43

LIST OF FIGURES

Figure No.	Title	Page
1	Skewed Rigid-Frame Bridge Model	11
2	a. Deck Reinforcing	12
	b. Abutment Reinforcing	13
	c. Cross-Section Perpendicular to Abutments	14
3	Model Form and Reinforcing Before Pouring	15
4	Strain Gage Position	16-17
5	Reaction Dynamometers	20
6	Detail of Reaction Dynamometer Parts	21
7	Testing Frame and Model	22
8	Variation of Strain for Longitudinal Reinforcing	36
9	Direction and Magnitude of Principal Stresses for Gages 3CID and 3COD (N., E., S., W.).	39

LIST OF TABLES

		Page
Table I	Strain Gage Positions.	24
Table II	Physical Properties of Concrete.	28
Table III	Dynamometer Strains for 160 lb. Load.	32
Table IV	a. Unit Strain in Longitudinal Reinforcing Steel for 160 lb. Load.	32
	b. Unit Strain in Transverse Reinforcing Steel for 160 lb. Load.	33
	c. Unit Strain in Rosette Gages for 160 lb. Load.	33
Table V	Magnitude and Direction of Principal Stresses for Gages 3CID and 3COD (N., E., S., W.).	35
Table VI	Deflection	35

SYMBOLS

E = Young's Modulus

ν = Poisson's Ratio

σ_{\max} = Maximum Principal Stress

σ_{\min} = Minimum Principal Stress

ϵ_{\max} = Maximum Principal Strain

ϵ_{\min} = Minimum Principal Strain

ϕ = Angle of Orientation of Maximum Principal Stress

ϵ_x = Strain Along x-Axis

ϵ_y = Strain Along y-Axis

ϵ_{xy} = Shear Strain

$\epsilon_{\theta_1}, \epsilon_{\theta_2}, \epsilon_{\theta_3}$ = Strain Readings Obtained From Rosette Gages

INTRODUCTION

In the past, engineers have found that the rigid frame bridge is more economical, has greater simplicity, and is more adaptable to architectural treatment than the conventional deck or through girder bridge. From the highway engineer's point of view, the rigid frame bridge also offers a preferable solution to the problem of grade separation. This explains why structures of this type have been so extensively used throughout the United States.

Fast experience indicates that the skewed rigid-frame bridge is a more adaptable type of structure, especially for modern traffic engineering design. Early theories of skewed rigid-frame structures were based on the same assumptions that had previously been used for unskewed slab bridges, but these proved inadequate. The recent theories⁽¹⁾ developed are more accurate and take the skew into account, but are not based upon a thorough elastic analysis. The analytical procedures used at the present time for calculating the actual stresses in the deck of a skewed rigid-frame bridge are based on the assumption that the torsional moments in the deck will twist it as though it were a thin rectangle of constant depth, whereas the bridge is actually haunched and the cross-section at the supporting abutment is not perpendicular to the longitudinal axis of the deck. As a result there is a considerable doubt as to the actual stresses that do develop under loading conditions.

An exact solution for a folded skewed plate has been developed by Dr. Daniel Frederick⁽²⁾ and detailed calculations are now being made. This solution will be compared with the results of an earlier

experimental study⁽³⁾ but will not include the effect of haunching nor of composite material so characteristically used in reinforced concrete structures.

It is, therefore, the purpose of this research to build an experimental model of an existing reinforced concrete skewed bridge⁽⁴⁾ to a one-tenth scale and to subject this to various loading conditions. This thesis outlines the experimental procedure followed in testing this model and lists the results obtained. SR-4 strain gages were used to measure the strains in the reinforcing steel and on the surface of the concrete itself at selected points. The model was loaded with concentrated load at the center of the deck keeping all strains within the elastic limit of the materials.

Later tests will test the model with the load placed at eight other positions on the deck. The model will finally be tested to destruction under a uniform load applied by means of a hydraulic rubber cell fitted to the top of the deck surface, but these results are not included in this thesis.

REVIEW OF LITERATURE

The experimental investigation of skewed rigid frame bridges has received very little attention in the past and only a few of such tests are discussed in the literature. These can be classified into two parts and are described below.

1. Model Tests.

In 1932, model tests on a skewed rigid frame bridge were conducted by E. F. Gifford⁽⁵⁾. The model used had a 45° skew, was constructed of concrete and had a scale ratio of prototype to model of 64. The model was tested to destruction with the concentrated loads at the center and quarter points but only the appearance and description of cracks were noted. Photographs indicated that failure occurred at the top of the slab for both symmetrical and unsymmetrical loads. The first crack continued approximately perpendicular to the traffic. Gordon P. Fisher and Walter C. Boyer⁽⁶⁾ conducted a number of tests on a model of a skewed bridge with a two-span rigid frame in an attempt to obtain the reactions. The effect of skew on the reaction was investigated for angles varying from 0° to 50° in increments of 10° . The deck was flat and of constant thickness. This investigation was based on the deformer method as developed by Beggs and modified by William J. Eney.

2. Full Size Tests.

Some tests on existing structures were made. The literature revealed that full size tests were made on the Central Avenue Bridge, Glendale, California⁽⁷⁾ and the North Avenue Bridge, Chicago, Illinois⁽⁸⁾.

a. Central Avenue Bridge, Glendale, California.

This bridge was made available for tests of the full scale structure in 1939. It was designed by the Hayden method and had a solid deck. When tested the structure was two years old. Steel ingots weighing 3,000 lb. each were spread at various distances along the transverse center line in a strip three feet wide. Strains were measured at the haunch and crown with 10 inch Whittemore and 2 inch Berry strain gages attached to the exposed reinforcing rods. Dial gages were used to measure the deflections of the corners of the deck, crown, and bottom of the abutments. The results indicated that the maximum stress occurred in the tension steel at the obtuse corner, that the entire structure rotated as a rigid body, and that the maximum deflection of the crown under the greatest load (440 tons) was approximately $3/8$ inches.

b. North Avenue Bridge, Chicago, Illinois.

This bridge was a two hinged rigid frame of slab and girder design with hinges tied by reinforcing to the lower roadway slab. The bridge had a 55° skew. Special extensometer stations were built into the deck girder, one tie slab and the abutments. Temperature variations over a period of four months and their effect on hinge movements and deck deflections were recorded. As the result of these tests it was concluded that torsional effects were negligible for this T-beam type deck and that the structural behavior was in good agreement with the assumed action. It should be noted, however, that this was not a flat slab-type structure.

EXPERIMENTAL INVESTIGATION

1. Object of the Investigation

The purpose of this thesis is to obtain experimental data on the behavior of a skewed haunched-slab rigid-frame bridge so that these strains and deflections may later be compared with the results of a theoretical analysis based on a rigorous treatment involving the theory of elasticity. The laws of similitude were applied keeping the stresses and strains equal between model and prototype. Preliminary experimental studies at V. P. I. were carried out in the past⁽⁹⁾ indicating that small reinforced concrete models of reinforced concrete beams and slabs did follow the theoretical laws of similitude.

2. Construction of the Model

The model is a one-tenth scale version of an existing prototype. Figure 1 shows its detailed dimensions, figures 2 and 3 the position of reinforcing, figure 4 the location of strain gages, etc. It should be noted that one-eighth inch diameter deformed wire was used for the reinforcing bars throughout most of the structure and that this had been found to behave properly in previous tests that were made on a skewed slab⁽³⁾. The spacing of the model reinforcing bars was computed keeping the steel ratio per unit area at each section the same as that used in the prototype. The only variation occurred in the vertical steel on the front face of the abutment where one-sixteenth smooth diameter bars had to be used in order to keep the spacing reasonable.

Type A-7 SR-4 strain gages were connected to the one-eighth inch

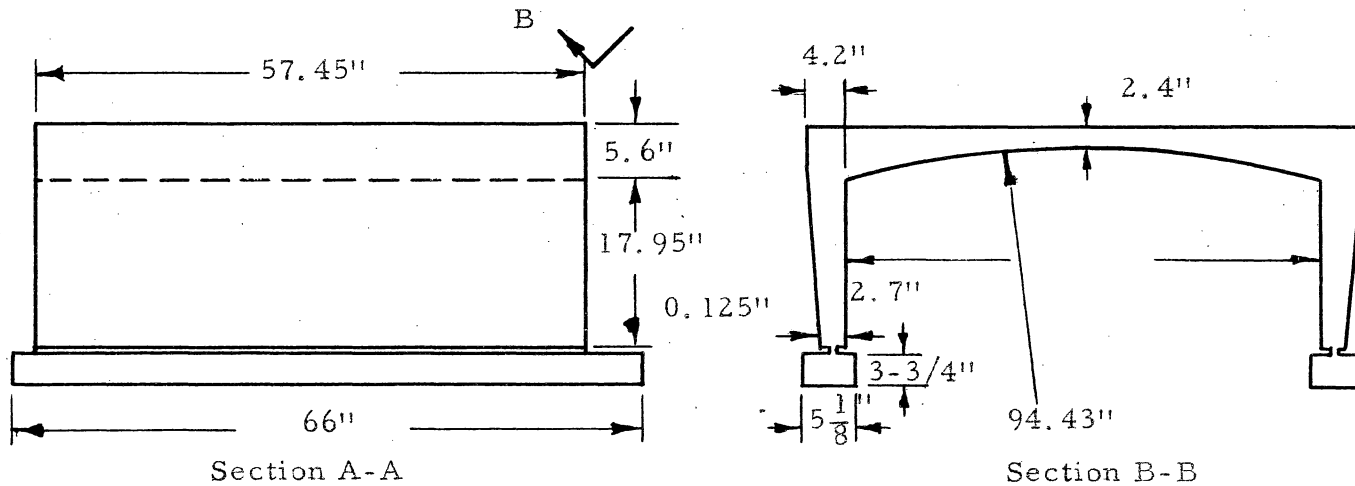
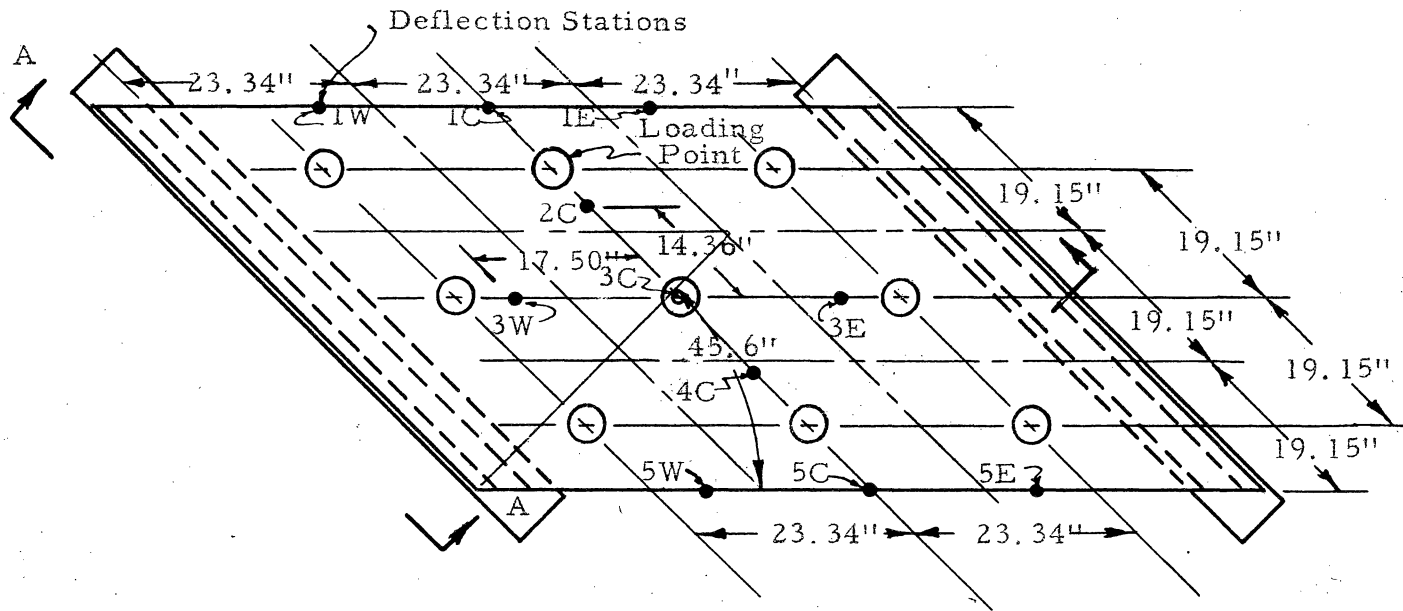
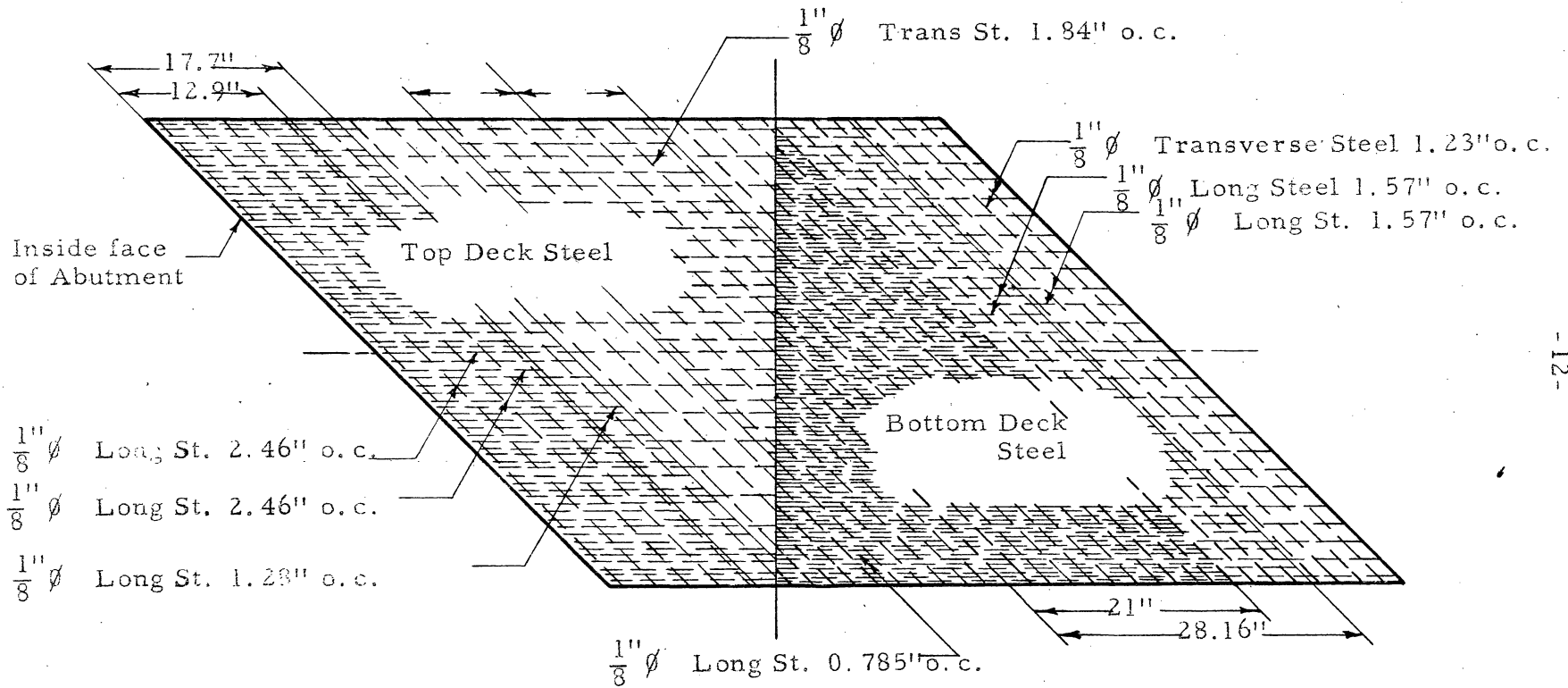


FIGURE 1
SKEWED RIGID-FRAME BRIDGE MODEL



0 3 6 9 12 15
 Scale in Inches

FIGURE 2 a
 Deck Reinforcing

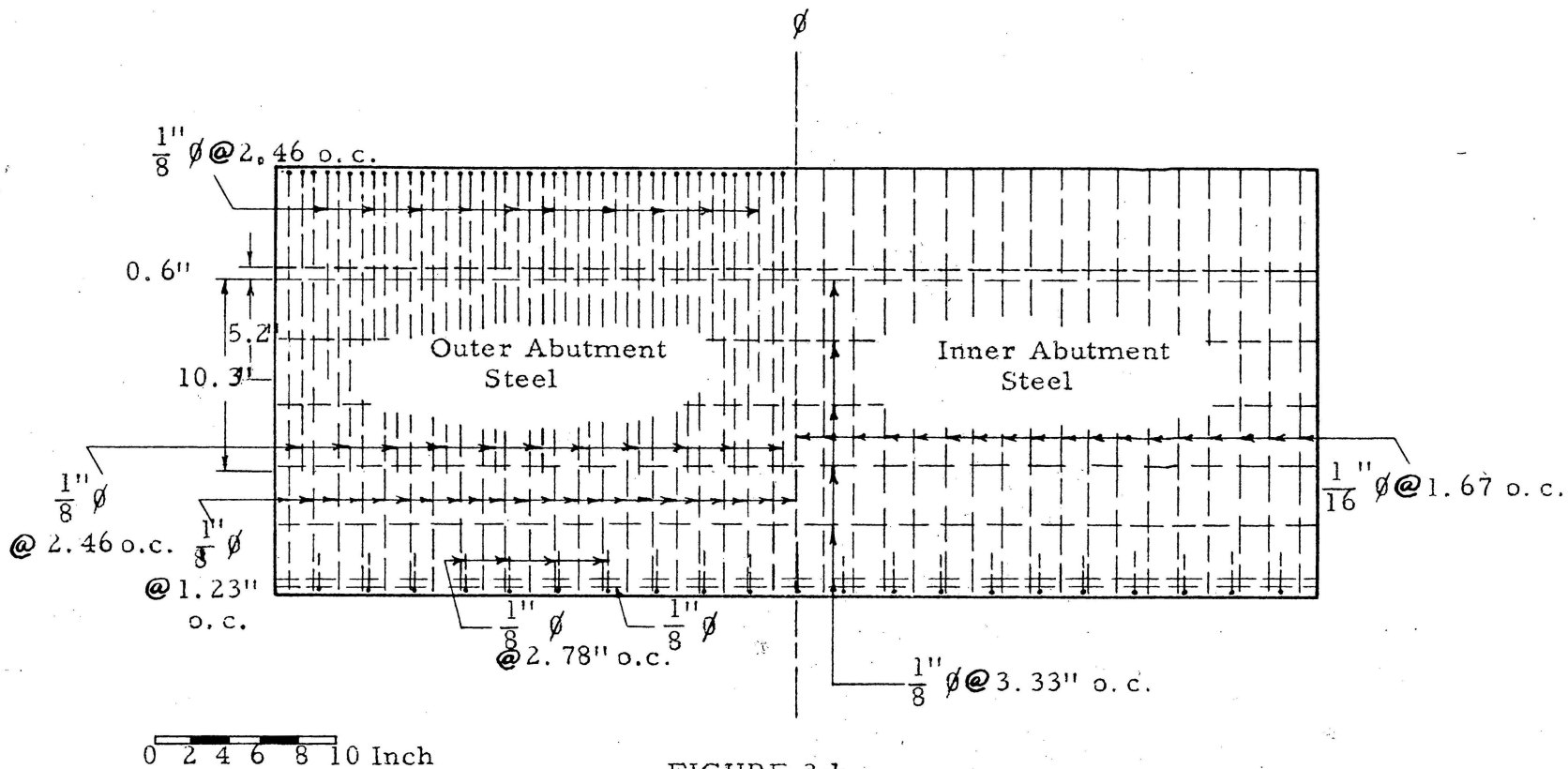


FIGURE 2 b
Abutment Reinforcing

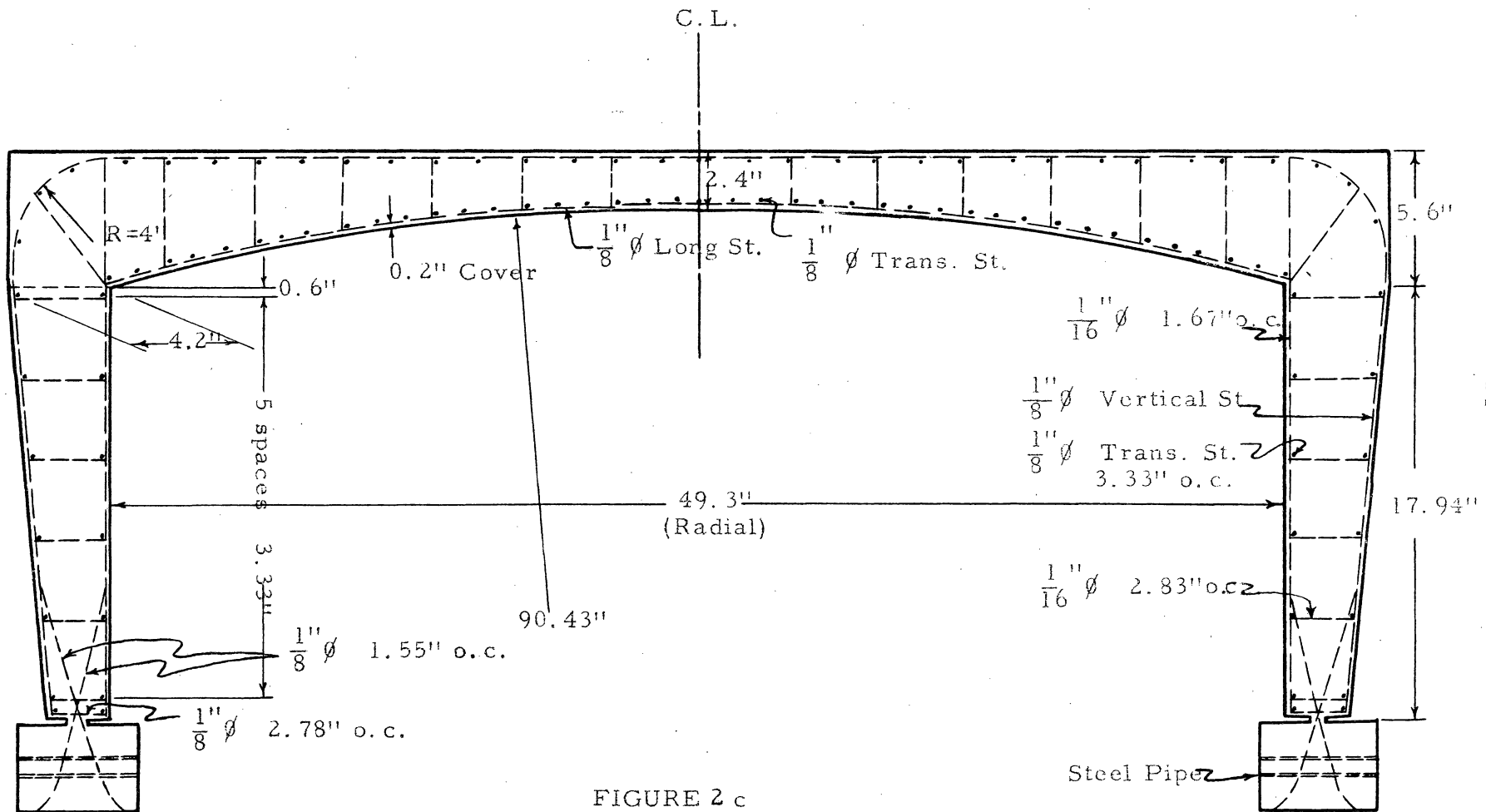


FIGURE 2 c

Cross-Section Perpendicular to Abutments

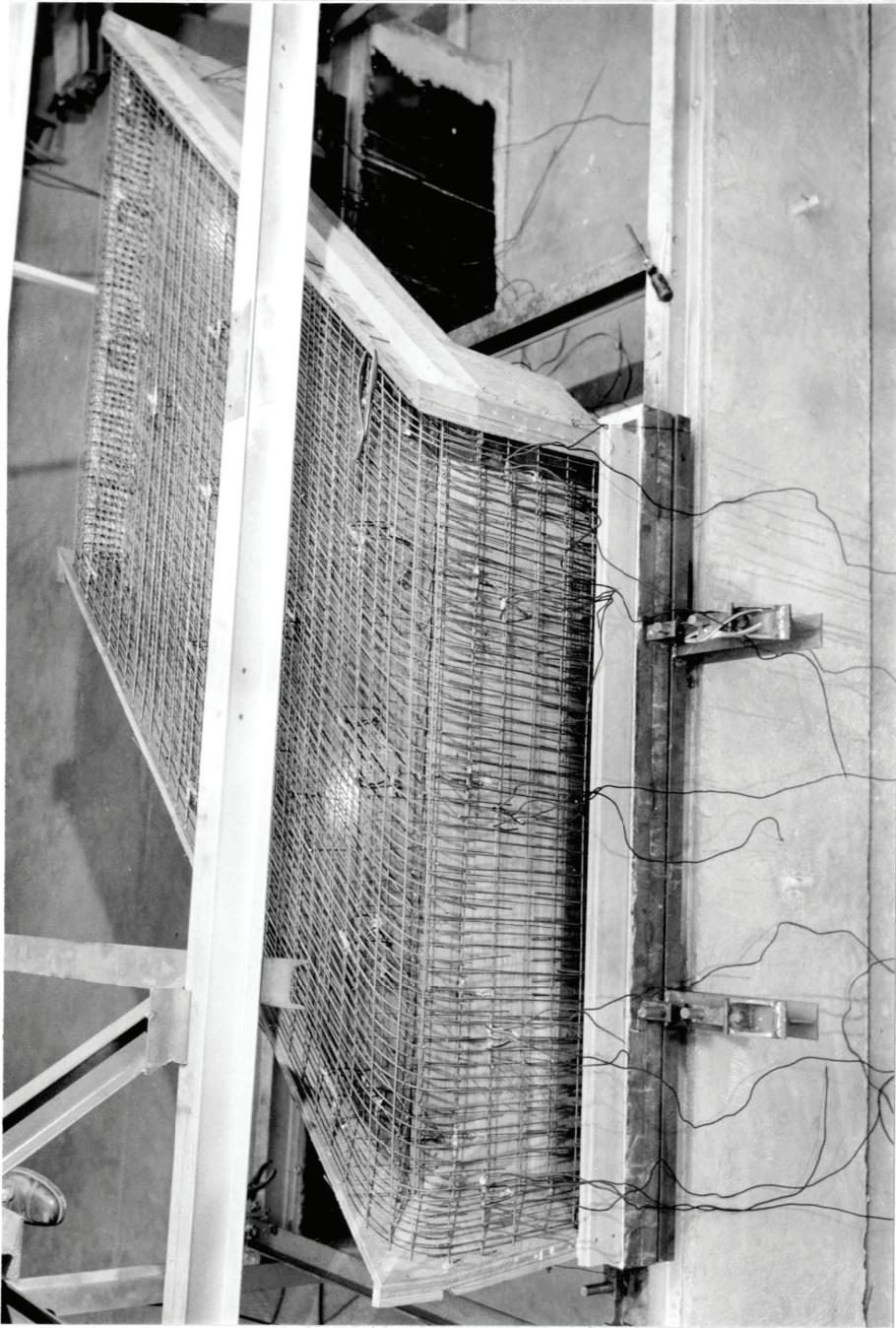


Figure 3 Model Form and Reinforcing before Pouring

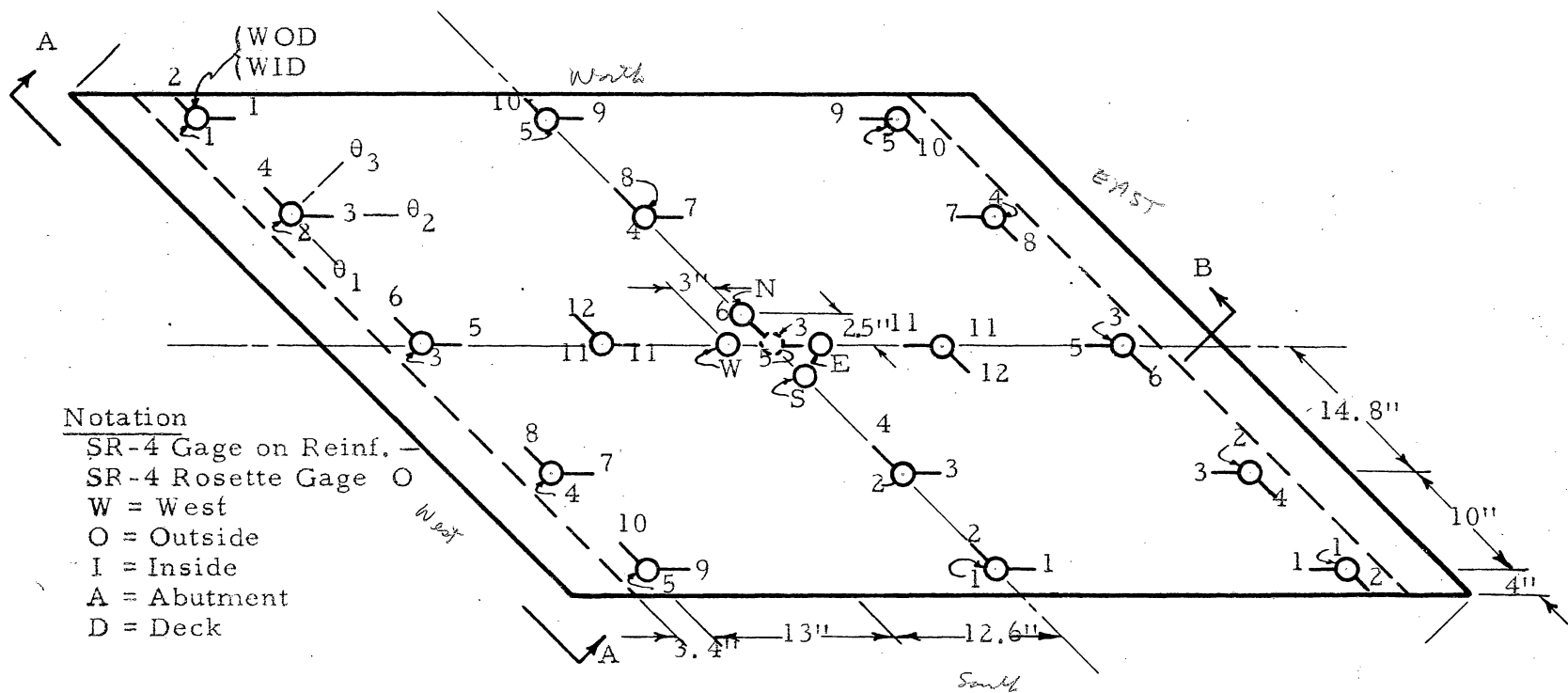
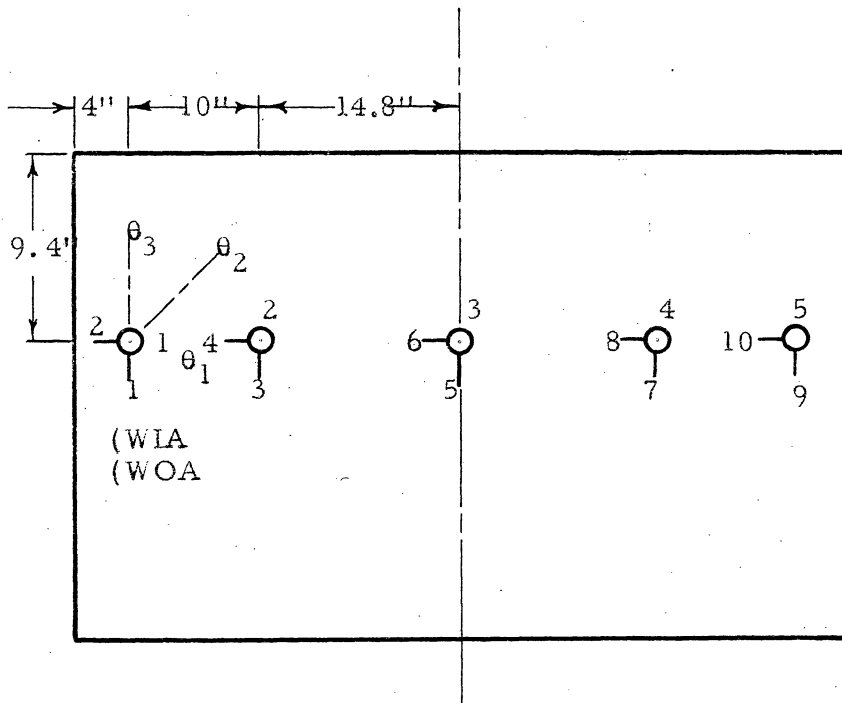
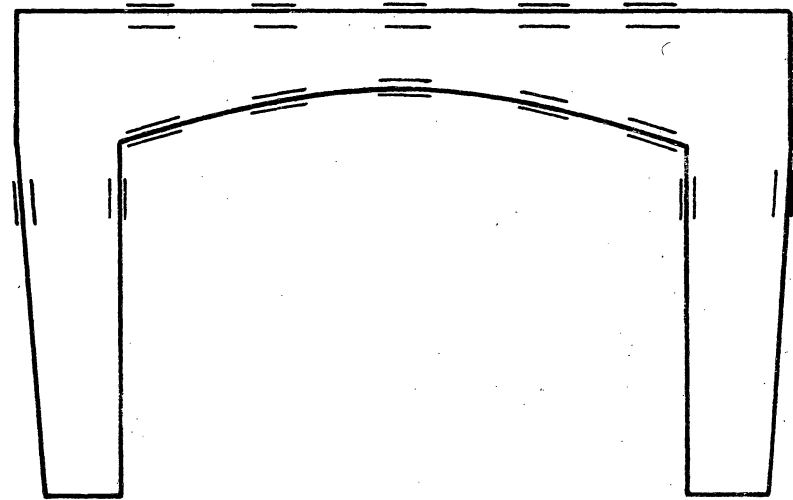


FIGURE 4 a
Strain Gage Position in Deck



Section A-A



Section B-B

FIGURE 4 b
Strain Gage Position in Abutment

reinforcing and type A-7-4 SR-4 strain gages were fastened to the one-sixteenth inch reinforcing. Type AR-2 rosette SR-4 strain gages were used on the top and bottom surfaces of the concrete deck and front and back faces of the abutments. Their location is indicated in figure 4 and Table I. Strain gages attached to the reinforcing were waterproofed with several layers of Armstrong Adhesive A-2, and then wrapped with rubber tape.

The bridge footings were cast in two steel boxes as indicated in figure 5. This arrangement was used in order to obtain greater rigidity of the footings so that the horizontal reactions developed by the various loads could be measured with the dynamometers indicated on this sketch.

The concrete used for the model contained 6.89 sacks per cubic yard and 8.7 gallons per sack. This gave a seven day strength using high early strength cement of 4757 psi, a modulus of elasticity of 3.61×10^6 psi, and a Poisson's ratio of 0.189. The mix had a five inch slump and so was easily placed in the form. The strength was determined from 2 x 4 inch cylinders. Table II indicates the properties of this mix as tested under standard conditions and also indicates the results obtained from companion cylinders cured in a manner identical with that of the model itself. The model and these cylinders were cured in their molds for five days, the molds then stripped, and then subjected to the normal dry air of the laboratory during the remainder of the test period.

3. Testing Frame

The model was placed in the testing frame shown in figure 7 and loaded with a hydraulic jack. The load was measured with an SR-4

type Baldwin Load Cell.

Horizontal reactions of each footing were measured with three dynamometers as indicated in figure 5 and figure 6. The steel channel box housing the footing was placed on ball bearings to eliminate friction. Rotation of the footing about its longitudinal axis was not noted but could easily have been prevented with small I-bar anchorages at each corner placed in a vertical position.

METHOD OF TESTING

1. Loading.

The model was investigated for stress distribution due to the concentrated load at various points on the deck. The surface of the deck was divided into nine panels by the equi-spaced lines as shown in figure 1. This thesis lists the results obtained for the concentrated load applied at the center of the middle panel; i. e., the center of the deck. The concentrated load was applied by using a 10,000 lb. hydraulic jack. In order to prevent a punching shear failure a 2 inch diameter steel cylinder was used under the load cell, and this was separated from the model by a soft rubber cushion to eliminate uneven bearing.

2. Measurement of Strains.

Since there were ninety-eight type A-7 SR-4 strain gages, ten type A-7-4 SR-4 strain gages, and fifty-seven type AR-2 rosette SR-4 strain gages on the reinforced concrete model, and since the switching and balancing units could carry a maximum of sixty-six gages at one time, it was necessary to divide these into groups and to test the model

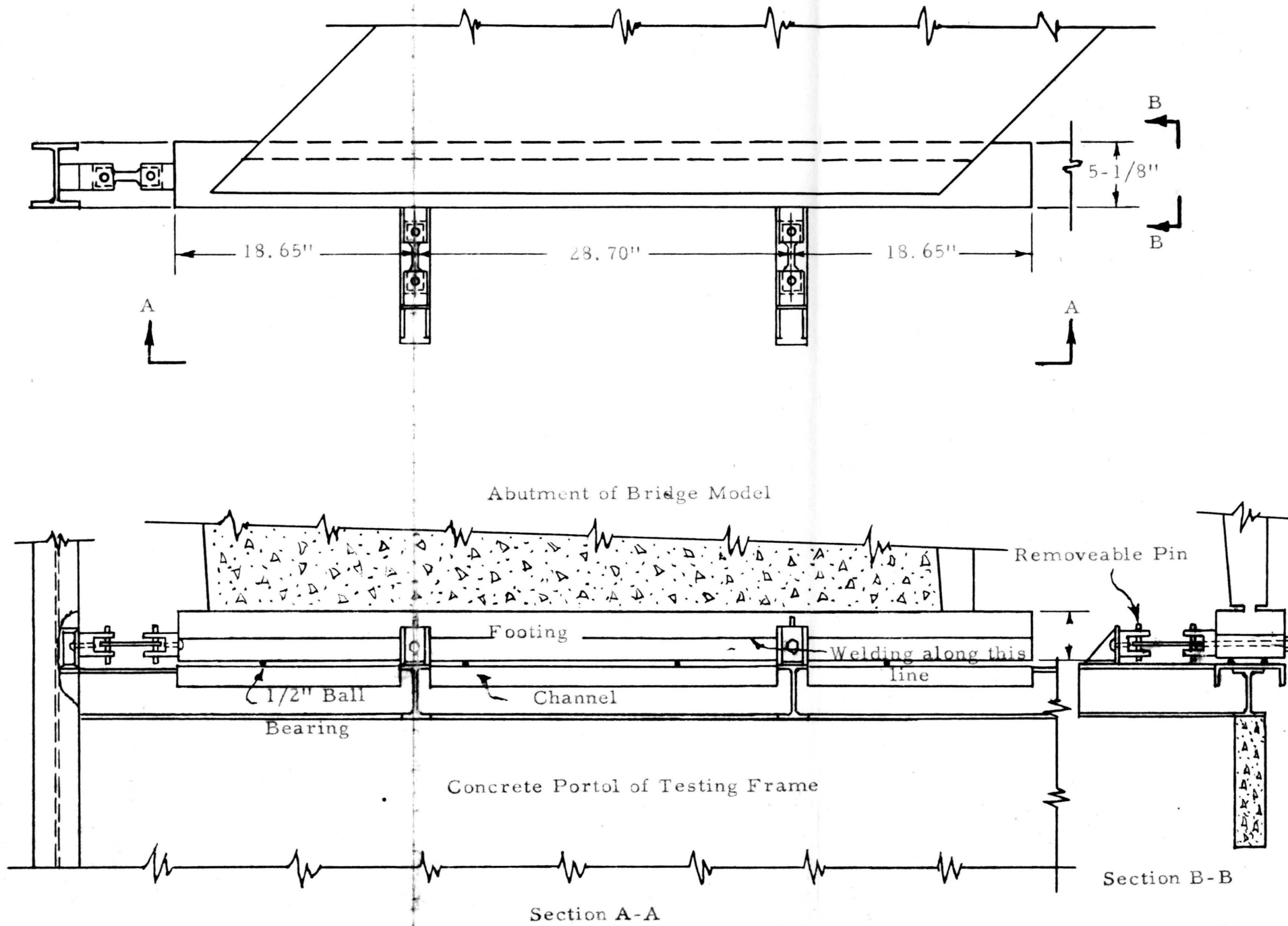


FIGURE 5
Reaction Dynamometers

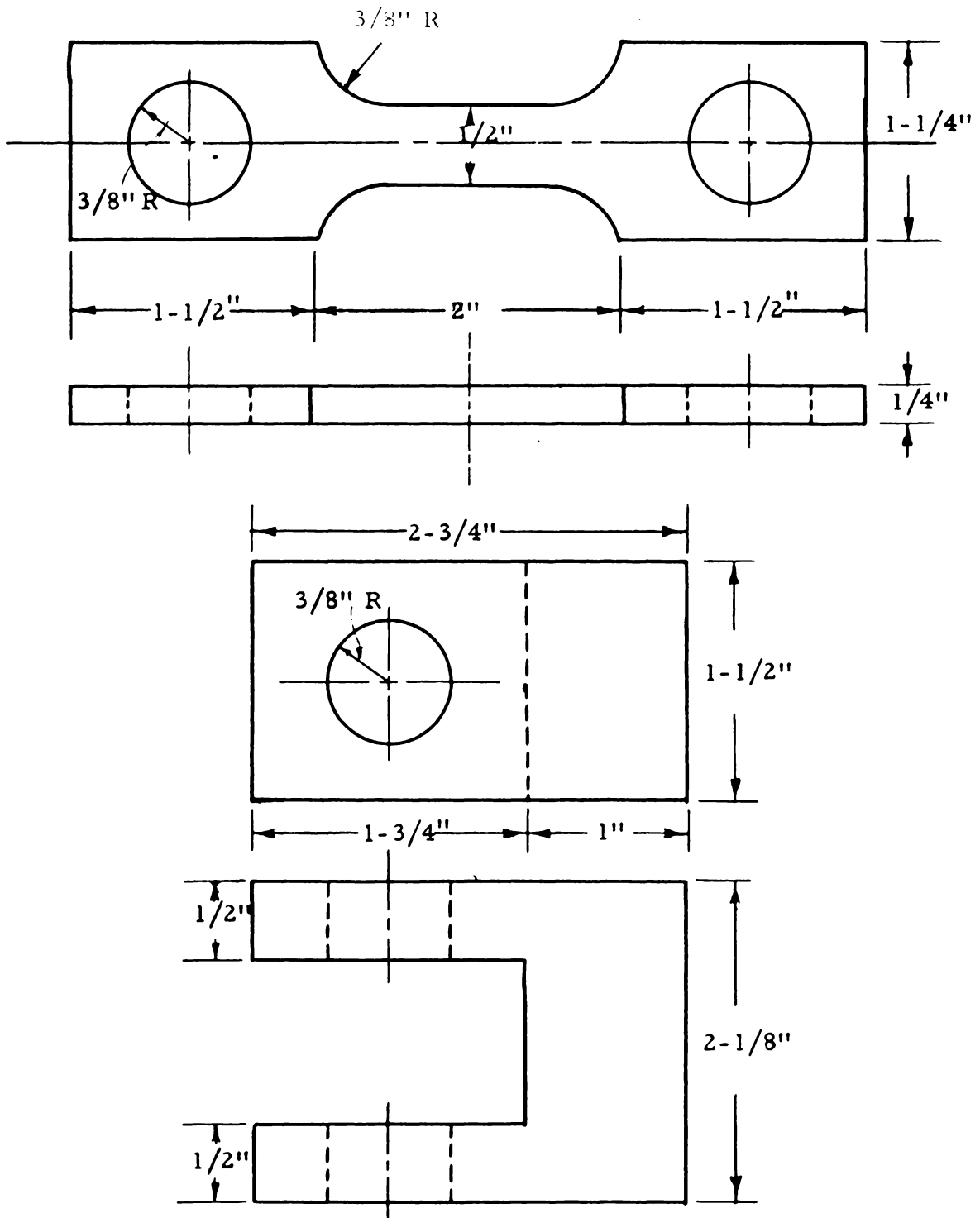


FIGURE 6
DETAIL OF REACTION DYNAMOMETER PARTS

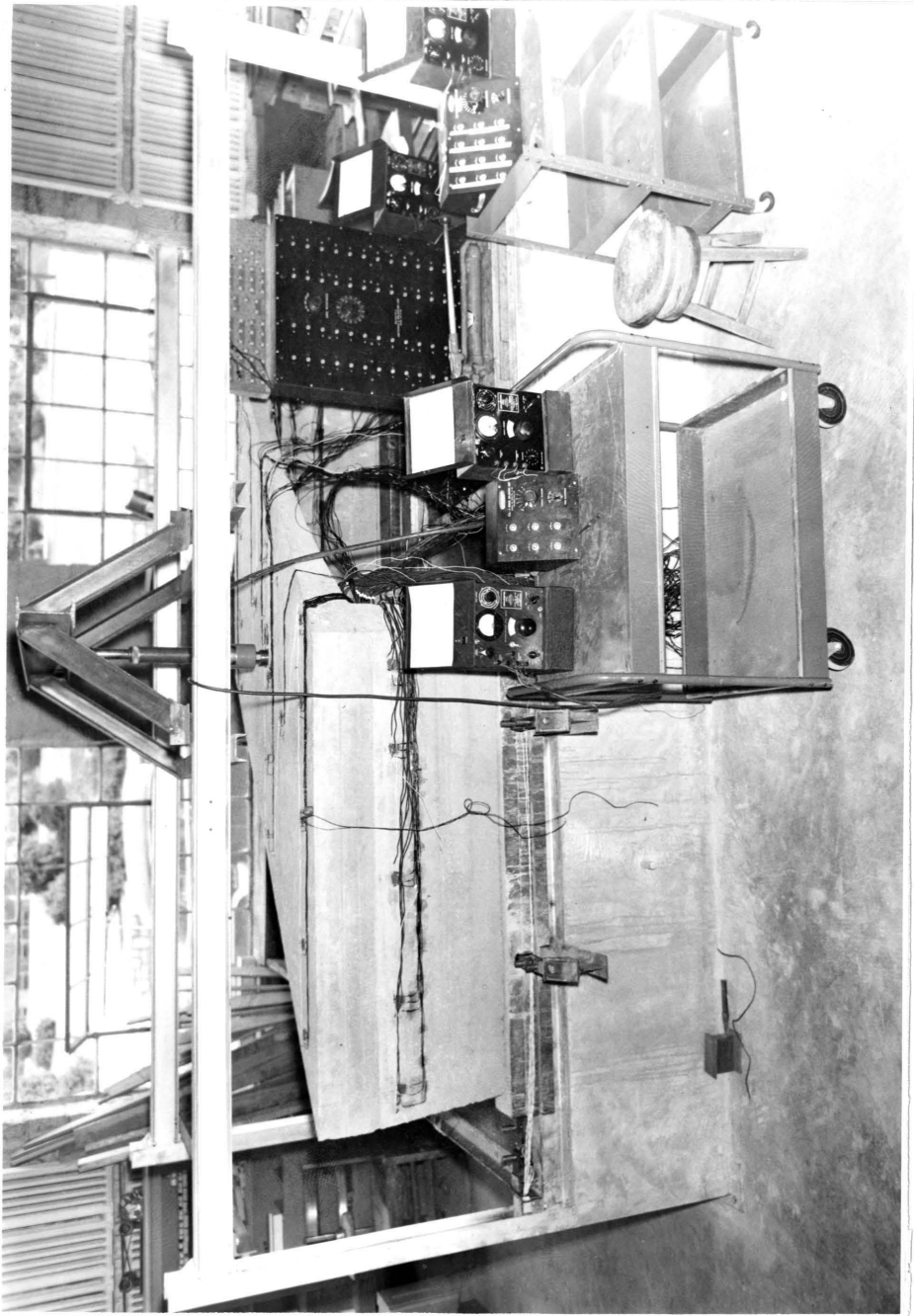


Figure 7 Testing Frame and Model

five times for each load. Rewiring of the switching and balancing units after each series of gages were read was eliminated by using a multi-plug system. The switching and balancing unit was permanently connected to the base of the multi-plug and socket unit and to the strain indicator. The ground lead and the compensating gage were connected directly to the switching and balancing unit. Six gages, No. 5CID, 6CID, 9WOA, 9WOD, 9EOA, 9EOD, were always connected to a separate switching and balancing unit for the special purpose of checking these readings for series of the five loadings.

3. Measurement of the Deflection of the Deck.

The deflection of selected points of the deck, as indicated in figure 4, was read on Ames dials reading to 0.001 inches.

4. Measurement of the Load and Reactions.

The applied load was measured by means of a Baldwin load cell as is indicated in figure 7. The horizontal thrust was measured by six SR-4 type dynamometers attached to the two footings.

REINFORCING

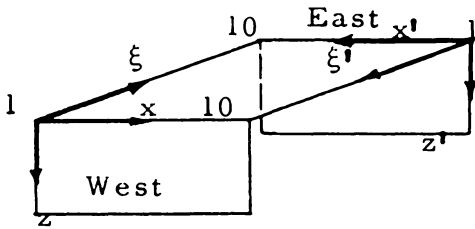
The reinforcing was obtained from the American Steel and Wire Company. The physical properties of this 1/8 inch diameter deformed wire were as follows:

Physical Properties of 1/8" ϕ Reinforcing Steel

Modulus of Elasticity	29,050,000 psi
Ultimate Stress	63,900 psi
Johnson's Elastic Limit	39,200 psi
Prop. Limit	24,800 psi
Yield Strength	51,000 psi
% e in 2"	18.0
% R. A.	76.0

TABLE I

(a)



Note: Coordinate d for any gage is measured to the nearest surface of the bridge perpendicular to the outer surface of either the abutment or deck.

Gage	Position Coordinates in Inches		
	x	ξ	d
1WOD	3.90"	9.10"	0.25"
2WOD	1.50"	9.50"	0.50"
3WOD	14.00"	9.20"	0.25"
4WOD	13.75"	9.50"	0.50"
5WOD	28.50"	9.50"	0.25"
6WOD	28.25"	9.50"	0.50"
7WOD	42.70"	9.60"	0.25"
8WOD	42.70"	9.50"	0.50"
9WOD	53.00"	9.80"	0.25"
10WOD	52.50"	9.50"	0.50"
1WID	3.10"	9.20"	0.20"
2WID	2.00"	9.50"	0.45"
3WID	14.20"	9.30"	0.20"
4WID	13.65"	9.50"	0.45"
5WID	28.80"	9.40"	0.20"
6WID	28.60"	9.50"	0.45"
7WID	42.80"	9.60"	0.20"
8WID	43.00"	9.50"	0.45"
9WID	53.30"	9.70"	0.20"
10WID	53.00"	9.50"	0.45"
	x	d	z
1WOA	4.00"	0.20"	9.40"
2WOA	4.50"	0.45"	9.70"
3WOA	14.60"	0.20"	9.40"
4WOA	14.70"	0.45"	9.80"
5WOA	28.70"	0.20"	9.40"
6WOA	29.30"	0.45"	9.70"
7WOA	44.40"	0.20"	9.70"
8WOA	44.50"	0.45"	9.40"
9WOA	55.00"	0.20"	9.40"
10WOA	55.00"	0.45"	9.40"

TABLE I (continued)
(a)

Gage	Position Coordinates in Inches		
	x	d	z
1WIA	3.40"	0.20"	9.70"
2WIA	3.30"	0.30"	9.40"
3WIA	14.20"	0.20"	9.70"
4WIA	13.80"	0.30"	9.40"
5WIA	29.00"	0.20"	9.70"
6WIA	29.00"	0.30"	9.40"
7WIA	43.80"	0.20"	9.70"
8WIA	43.60"	0.30"	9.40"
9WIA	54.80"	0.20"	9.70"
10WIA	55.00"	0.30"	9.40"
	x	ξ	d
11WOD	28.50"	25.30"	0.25"
12WOD	27.80"	25.30"	0.50"
11WID	28.90"	25.30"	0.20"
12WID	28.00"	25.30"	0.45"
1COD	3.90"	40.00"	0.26"
2COD	2.60"	41.00"	0.40"
3COD	14.40"	40.25"	0.24"
4COD	15.30"	41.00"	0.46"
5COD	28.70"	41.00"	0.26"
6COD	29.70"	41.00"	0.43"
7COD	43.00"	40.50"	0.26"
8COD	43.90"	41.00"	0.43"
9COD	53.00"	41.00"	0.26"
10COD	54.75"	41.00"	0.46"
1CID	4.30"	40.00"	0.20"
2CID	2.60"	41.00"	0.50"
3CID	14.80"	40.30"	0.21"
4CID	15.30"	41.00"	0.48"
5CID	29.20"	40.40"	0.22"
6CID	29.90"	41.00"	0.50"
7CID	43.10"	40.00"	0.20"
8CID	44.20"	41.00"	0.50"
9CID	52.90"	40.50"	0.22"

TABLE I
(b)

Gage	Position Coordinates in Inches		
	x'	ξ'	d
1EOD	4.00"	9.40"	0.28"
2EOD	4.18"	9.60"	0.40"
3EOD	14.30"	9.20"	0.25"
4EOD	12.69"	9.60"	0.40"
5EOD	28.40"	9.80"	0.30"
6EOD	27.80"	9.60"	0.43"
7EOD	42.70"	9.60"	0.25"
8EOD	42.00"	9.70"	0.38"
9EOD	53.20"	9.60"	0.25"
10EOD	53.70"	9.60"	0.38"
1EID	4.00"	9.40"	0.20"
2EID	3.50"	9.60"	0.45"
3EID	14.60"	9.30"	0.22"
4EID	13.80"	9.60"	0.50"
5EID	28.40"	9.80"	0.21"
6EID	29.20"	9.60"	0.50"
7EID	42.10"	9.80"	0.28"
8EID	43.00"	9.60"	0.52"
9EID	53.20"	9.70"	0.25"
10EID	54.50"	9.60"	0.51"
	x'	d	z'
1EOA	4.25"	0.20"	9.90"
2EOA	3.50"	0.33"	9.90"
3EOA	14.50"	0.20"	9.80"
4EOA	14.00"	0.33"	9.40"
5EOA	29.50"	0.20"	9.80"
6EOA	28.80"	0.33"	9.40"
7EOA	44.60"	0.20"	9.90"
8EOA	43.70"	0.33"	9.40"
9EOA	55.00"	0.20"	9.90"
10EOA	54.20"	0.33"	9.40"
1EIA	3.50"	0.20"	9.70"
2EIA	2.50"	0.30"	9.40"
3EIA	13.50"	0.20"	9.70"
4EIA	13.00"	0.30"	9.40"
5EIA	28.70"	0.20"	9.70"
6EIA	28.30"	0.30"	9.40"
7EIA	43.00"	0.20"	9.70"
8EIA	42.50"	0.30"	9.40"
9EIA	54.00"	0.20"	9.70"
10EIA	54.00"	0.30"	9.40"

TABLE I (continued)
(b)

Gage	Position Coordinates in Inches		
	\bar{x}'	$\bar{\xi}'$	d
11EOD	28.50"	25.10"	0.22"
12EOD	28.00"	25.00"	0.40"
11EID	28.70"	25.00"	0.23"
12EID	28.00"	25.40"	0.49"

TABLE II

Curing	Age in Days	Ult. Strength (f_c) in psi.	Sec. Mod. of Elas. (E) in psi. at 1350 psi.	Poisson's Ratio	Batch No. Cycl. No.
Molds-1 day	7	4920	3.91×10^6		3/3
100% R.H., 75°F-4 days		4700	3.20×10^6		6/2
50% R.H., 70°F-2 days		4650	3.73×10^6	0.189	6/3
		Av. 4757	Av. 3.61×10^6		
Molds-5 days	7	4620	3.28×10^6		2/1
Thence open		4510	3.88×10^6		2/3
storage in lab.		4540	3.26×10^6	0.186	5/1
air.		Av. 4557	Av. 3.44×10^6		
Molds-5 days	14	4830	3.62×10^6		3/1
Thence open		5250	3.78×10^6		4/2
storage in lab.		4150	4.10×10^6		5/3
air.		Av. 4750	Av. 3.83×10^6	0.197	
Molds-5 days	28	5140	3.39×10^6		6/1
Thence open		5690	3.43×10^6		5/2
storage in lab.		5320	3.91×10^6	0.210	4/1
air.		Av. 5380	Av. 3.58×10^6		

DATA AND RESULTS

1. Stress and Strain in the Reinforcing.

At each selected point, two SR-4 strain gages were attached to the transverse and longitudinal reinforcing. Since the gages were not exactly coincident the strains at any selected point can be determined by interpolation. The procedure would be to plot the strains (ϵ_x and ϵ_y or ϵ_z) versus their location along the section as in figure 8. The strain at any point could be found from this curve.

After this, the corresponding stress could be calculated by applying the stress equation $\sigma = E\epsilon$ where E is the elastic modulus of the reinforcing. The depth of the reinforcing bars at each gage position is given in Table I.

2. Calculation of Principal Strains from the Type AR-2 Rosette Gages.

a. Derivation of Equations.

When a surface element is subjected to the combined action of strains ϵ'_x , ϵ'_y and ϵ'_{xy} the strain ϵ_θ in the longitudinal direction of θ is given by the equation

$$\epsilon_\theta = \epsilon_x \cos^2 \theta + \epsilon_y \sin^2 \theta + \epsilon_{xy} \sin \theta \cos \theta$$

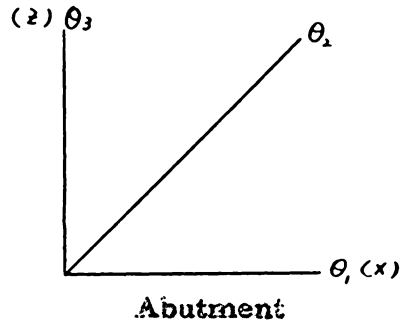
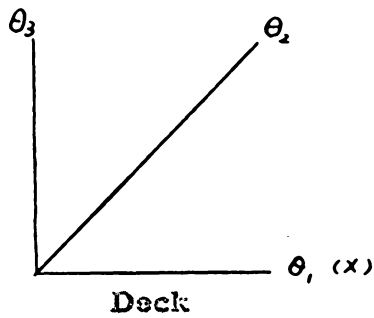
The magnitude and direction of the maximum and minimum principal strains can be determined by the following relations

$$\epsilon_{\max} = \frac{1}{2} \left[(\epsilon_x + \epsilon_y) + \sqrt{(\epsilon_x - \epsilon_y)^2 + \epsilon_{xy}^2} \right]$$

$$\epsilon_{\min} = \frac{1}{2} \left[(\epsilon_x + \epsilon_y) - \sqrt{(\epsilon_x - \epsilon_y)^2 + \epsilon_{xy}^2} \right]$$

$$\tan 2\phi = \frac{\epsilon_{xy}}{\epsilon_x - \epsilon_y}$$

Angle ϕ is measured positive counter-clockwise from ϵ_{θ_1} to the direction of ϵ_{\max} .



The three rosette strains can be written as ϵ_{θ_1} , ϵ_{θ_2} and ϵ_{θ_3} . Since $\theta_1 = 0$, $\theta_2 = 45^\circ$ and $\theta_3 = 90^\circ$, the three simultaneous equations reduce to the following

$$\epsilon_{\theta_1} = \epsilon_x$$

$$\epsilon_{\theta_2} = \frac{1}{2} \left[(\epsilon_x + \epsilon_y) + \epsilon_{xy} \right]$$

$$\epsilon_{\theta_3} = \epsilon_y$$

Therefore, ϵ_x , ϵ_y , and ϵ_{xy} , the maximum and minimum principal strains can be determined by these equations.

The calculation of principal stresses from the principal strains is based on the assumption that the material follows Hooke's Law.

$$\epsilon_x = \frac{\sigma_x}{E} - \nu \frac{\sigma_y}{E}$$

$$\epsilon_y = \frac{\sigma_y}{E} - \nu \frac{\sigma_x}{E}$$

Simultaneous solution of these two equations yields the following in terms of principal stresses and strains.

$$\sigma_{\max} = \frac{E}{1 - \nu^2} \left\{ \epsilon_{\max} + \nu \epsilon_{\min} \right\}$$

$$\sigma_{\min} = \frac{E}{1 - \nu^2} \left\{ \epsilon_{\min} + \nu \epsilon_{\max} \right\}.$$

b. Test Results

Due to the fact that a small load of 160 lb. had to be used to avoid cracking of the concrete, only those gages in the vicinity of the load showed any appreciable strain. Data for all rosette gages and for the gages attached to the reinforcing along the longitudinal and transverse center lines are shown in Table IV a, b and c. Table III indicates the strains on the reaction dynamometers. The two strains recorded for each dynamometer need only be averaged and multiplied by E for steel to determine the reactions in pounds.

c. Nomographic Charts

The calculation of principal stresses and strains by use of the equation in section (a) is laborious. The mathematical error is sometimes inevitable. It is more convenient to use nomograph⁽¹⁰⁾ for the solution of these equations, or, after completion of the calculations using the rosette equation, the nomograph can be used for checking the results obtained from the computation to reduce errors.

No known nomograph exists at present for the values of E and ν for concrete. Hence, maximum and minimum strains and stresses were determined from the equations. These results are shown in Table V.

3. Deflection Measurements.

The deflection of eleven selected points of the deck, as located in figure 1, is indicated in Table VI below.

TABLE III
Dynamometer Strains for 160 lb. Load

Gage No.	Unit Strain x 10 ⁶		Gage No.	Unit Strain x 10 ⁶	
	a	b		a	b
1E	-16	-12	1W	-12	-5
2E	-2	-8	2W	-3	-7
3E	-7	-7	3W	-8	-8

TABLE IV a
Unit Strain in Longitudinal Reinforcing Steel for 160 lb. Load

Gage No.	Unit Strain x 10 ⁶	Gage No.	Unit Strain x 10 ⁶
5W OA	+2	5W IA	-8
5W OD	+2	5W ID	-3
11W OD	+2	11W ID	-2
5C OD	-17	5C ID	+21
11E OD	+1	11E ID	-2
5E OD	+2	5E ID	-5
5E OA	+3	5E IA	-9
9W OA	+4		
9W OD	+2		
1C OD	-5	1C ID	+2
3C OD	-10	3C ID	+7
5C OD	-17	5C ID	+21
7C OD	-9	7C ID	Short
9C OD	-3	9C ID	+6
9E OD	0		
9E OA	+10		

TABLE IV b

Unit Strain in Transverse Reinforcing Steel for 160 lb. Load

Gage No.	Unit Strain x 10 ⁶	Gage No.	Unit Strain x 10 ⁶
6WOA	0	6WIA	0
6WOD	0	6WID	0
12WOD	-1	12WID	0
6COD	-15	6CID	5
12EOD	Short	12EID	0
6EOD	0	6EID	0
6EOA	0	6EIA	0
2COD	-2	2CID	0
4COD	0	4CID	Short
6COD	-15	6CID	5
8COD	no balance	8CID	0
10COD	Short	10CID	-1

TABLE IV c

Unit Strain in Rosette Gages for 160 lb. Load

Gage No.	Unit Strain x 10 ⁶			Gage No.	Unit Strain x 10 ⁶		
	e ₁	e ₂	e ₃		e ₁	e ₂	e ₃
1WOA	0	0	0	1WIA	0	-2	-6
2WOA	-2	0	0	2WIA	0	0	
3WOA	0	0	+2	3WIA	0	-8	-9
4WOA	-2	0	+2	4WIA	0	-9	-13
5WOA	-2	+5	+11	5WIA	0	-8	-10
1WOD		0		1WID	0	0	0
2WOD		0		2WID	0	-3	-2
3WOD		+2	+2	3WID	0	-7	-2
4WOD	0	+3	+3	4WID	0	-8	-7
5WOD		+2	0	5WID		-3	-3
11WOD		0		11WID	0	-2	0
1COD		-5		1CID	-2	+2	+2
2COD		-10	-17	2CID	-1	+2	+17
3COD-N	-4	-21	-28	3CID	+48	+28	+70
3COD-S	-15	-21	-33	4CID	-2		
3COD-W	-12	-13	-23	5CID	-2		+2
3COD-E	-17	-17	-21	11EID	+1	0	+3
4COD							
5COD	0	-7	-10				
11EOD							

TABLE IV c (Continued)

Gage No.	Unit Stress x 10 ⁶			Gage No.	Unit Stress x 10 ⁶		
	θ_1	θ_2	θ_3		θ_1	θ_2	θ_3
1EOD			0	1EID	0	-3	-3
2EOD	0	+2	+2	2EID	0	-2	-8
3EOD	0	+2	+2	3EID	-1	-7	-4
4EOD		+5		4EID	0	-5	-5
5EOD				5EID	0	-5	-3
1EOA	-2	0	+2	1EIA	0	-3	-3
2EOA	-2	0	0	2EIA	-2	-6	-7
3EOA	-2	+2	+2	3EIA	-1	-8	-12
4EOA	-2	+2	+3	4EIA	-2	-8	-9
5EOA	-2	+4	+4	5EIA	0	-4	-9

TABLE V

Gage No.	Unit Strain $\times 10^6$		Unit Stress in psi		ϕ_x for σ_{max}
	ϵ_{max}	ϵ_{min}	ϵ_{max}	ϵ_{min}	
3CID	+91.85	+26.15	+365.31	+167.53	+125°14'
N3COD	- 3	-29	- 33.11	-111.38	- 11°19'
E3COD	-16.17	-21.83	- 77.28	- 94.31	- 22°30'
S 3COD	-14.64	-32.36	- 79.44	-132.79	+ 8°12'
W3COD	-10.39	-24.61	- 57.63	-100.42	+ 19°57'

TABLE VI

Station Number	Deflection in Inches $\times 1000$
1 W	1.25
C	2.50
E	2.25
2 C	2.70
3 W	3.00
C	3.50
E	3.00
4 C	2.80
5 W	2.25
C	2.40
E	1.25

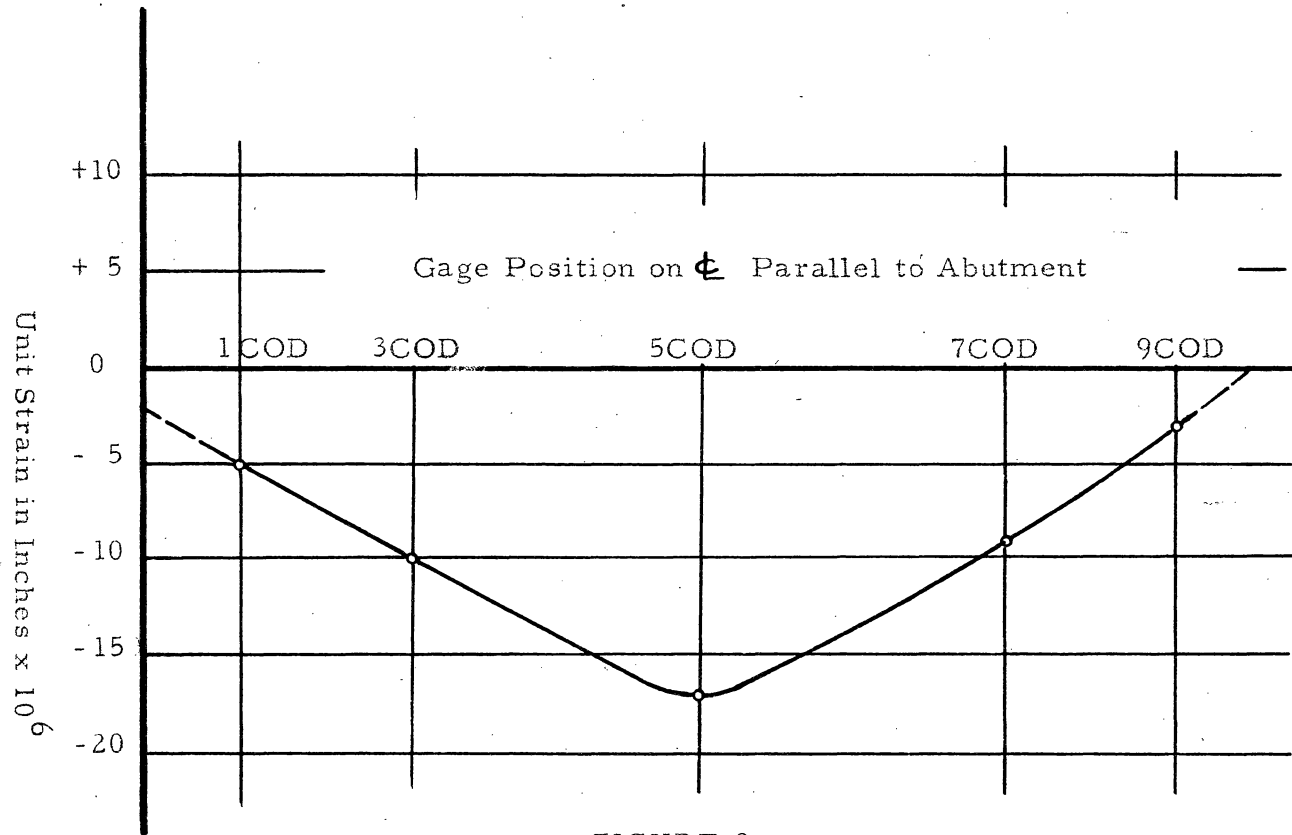


FIGURE 8
 Variation in Strain for Longitudinal Steel
 Along Parallel to the Abutment

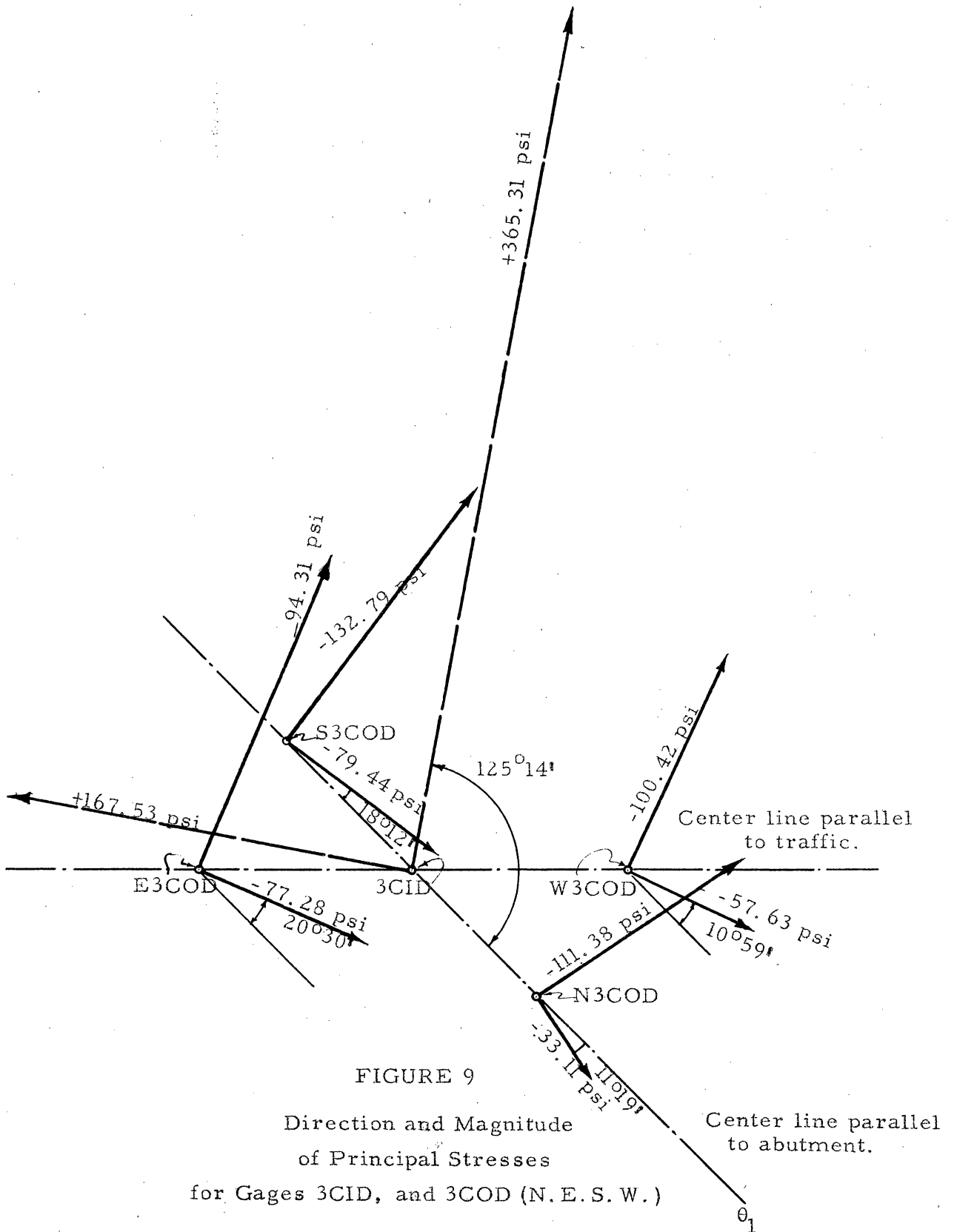


FIGURE 9
Direction and Magnitude
of Principal Stresses
for Gages 3CID, and 3COD (N. E. S. W.)

CONCLUSION

Since the building of this concrete model was a painstaking task the limited time made it impossible for this thesis to contain the complete data of this model test.

Though the testing load was light, the readings of strain gages in the center portion of the model still gave some significant results which justified the adequacy of the experiment. However, the author would like to make the following important conclusions:

a. The control of the accuracy in building the model is very important. All dimensions should be laid out as carefully as possible.

b. The placing of the SR-4 strain gages on small diameter reinforcing steel was difficult work. Attention should be paid not only to the problem of permeation of water, but also the technical skill to prevent short circuiting between the gage and the reinforcing steel. The performance of this type short-circuit would make it impossible to use a common neutral wire which connects all gages in the same series. In this condition, the only way to obtain correct readings of each gage was to measure the strains with individual load applications.

c. The multi-plug method is perfectly satisfactory. When the total number of strain gages is more than the switching and balancing unit can accommodate, using plugs of different color for different series would be very helpful during the test.

RECOMMENDATIONS

The author wishes to make the following recommendations for future work:

1. Measure the strain in all rosette gages and selected interior gages on the reinforcing for the 150 lb. load at the eight other load stations.

2. Repeat for a uniform load over the deck.

3. Use loads at the nine selected load stations heavy enough to stress the reinforcing to its working stress.

4. Protection of rosette gages on the top face of the deck during the uniform load test.

5. Strengthen the test frame for the heavy load.

6. Load up to ultimate with the uniform load.

7. Compare the results with an analytical study.

BIBLIOGRAPHY

1. Rathbun, J. C.: "Analysis of the Stresses in the Ring of a Concrete Skewed Arch"; Transactions, ASCE, Vol. 87 (1924), pp. 611-680.
"An Analysis of Multiple-Skew Arch on Elastic Piers", Transactions, ASCE, Vol. 98 (1933), pp. 11-14.
2. Frederick, Daniel: Unpublished, Memorandum of March 26, 1954 to members of Committee 314, Rigid Frame Bridges, American Concrete Institute.
3. Pletta, D. H. and Frederick, D.: "Model Analysis of a Skewed Rigid Frame Bridge and Slab", Journal of American Concrete Institute, Vol. 26, No. 3, November 1954, Proceedings, Vol. 51.
4. Brumer, Milton: "Comparative Designs of a Segmental Skewed Frame Concrete Bridge by the Straight Line and Plastic Theory Methods", Vol. XLV, 1949, pp. 409-419.
5. Gifford, E. F.: "Approximate Design Method for Concrete Rigid Frame", Engineering News Record, May 3, 1934.
6. Fisher, G. P. and Boyer, W. G.: "Reactions of a Two-Span Skewed, Rigid Frame Bridge", Highway Research Board, Research Report 14-B. p. 75.
7. "Unusual Bridge Test Involves Rigid Frame Built on Skew", Southwest Builder and Contractor, August 21, 1936. (Reprinted by Portland Cement Association.
"Unusual Concrete Rigid-Frame Test", Engineering News Record, November 17, 1938, pp. 615-617.
8. Smith, L. T. and Lillard, P.: "Extensometer Stress Measurements,

North Avenue Bridge, Chicago, Illinois", Transactions of the American Society of Civil Engineers, Vol. 107, (1942) pp. 1447-1469.

9. Pietta, D. H. and Frederick, D.: "Experimental Analysis", Proc. ASCE, Separate No. 224, July 1953.
10. Hewson, T. A.: "A Nomographic Solution to the Strain Rosette Equations", Experimental Stress Analysis, Vol. 4, No. 1 (1946), Addison-Wesley Press, Cambridge, Massachusetts, pp. 9-35.

ACKNOWLEDGMENT

The author wishes to express his gratitude to
who directed this research project and gave so much of his
valuable time in overcoming many technical and theoretical problems
encountered in this model test. The author is deeply indebted to
, Instructor of Applied Mechanics laboratory, for
his able help and precious suggestions in preparing the experimental
investigation.

Lastly, the author heartily thanks for her patient
and enthusiastic helping during the testing program.

**The vita has been removed from
the scanned document**